

# A comparison of the CCM1-simulated climates for pre-industrial and present-day CO<sub>2</sub> levels

Susan Marshall <sup>a,\*</sup>, Michael E. Mann <sup>b</sup>, Robert J. Oglesby <sup>c</sup>, Barry Saltzman <sup>b</sup>

<sup>a</sup> *Department of Geography and Earth Sciences, University of North Carolina, Charlotte, NC 28223, USA*

<sup>b</sup> *Department of Geology and Geophysics, Yale University, New Haven, CN, USA*

<sup>c</sup> *Department of Earth and Atmospheric Sciences, Purdue University, West Lafayette, IN, USA*

Received 21 June 1993; accepted after revision 16 February 1994

---

## Abstract

A comparison is made between the climatic equilibria of the NCAR CCM for a pre-industrial atmospheric CO<sub>2</sub> level (265 ppm) and a current (circa 1975) level of 330 ppm, including statistical estimates of the level of confidence in the implied changes. We also compare the model results to observations compiled over the past 100 years, which corresponds to roughly half of the period of change in CO<sub>2</sub> from pre-industrial (1800) to current levels. A relatively large model response in surface temperature and a smaller response in the precipitation, surface pressure, and storm track fields is obtained. These results are in accord with previous findings of the climate sensitivity to systematic changes in CO<sub>2</sub> forcings. A *t*-statistic of the model results indicates a significant surface temperature response to a relatively small change in CO<sub>2</sub>, above the inherent model variability.

Observations of global surface temperature anomalies for the period 1890–1990 show some similarities to the model results, especially a warming in regions of the wintertime northern hemisphere of 2–3° C. A point-by-point correlation of the 330 ppm minus 265 ppm model temperature differences to the observed 1980–1890 differences suggests that some of the variance in the observed trends in the surface temperature anomalies may be explained by the model experiments.

---

## 1. Prologue

Let us imagine that we are living in the year 1800 AD at the dawn of the industrial revolution when the atmospheric CO<sub>2</sub> concentration is lower than at present. We wish to investigate the climatic response to an increase in carbon dioxide from this present concentration to a projected increase to 330 ppm expected to occur by the year 1975. Imagine further that we have already achieved the level of expertise to construct a general circulation model such as the

CCM1 with which to assess the climatic response. What would our prediction of the climatic change have been (assuming the CCM1 results for 265 ppm accurately represent the 1800 AD climatic state)? How well would these changes have agreed with the observations? Would such a prediction have led us to any alarming projections for 1975 AD similar to the ones that are sometimes made currently for projected increase of CO<sub>2</sub> expected to occur by the year 2050? Most fundamentally, would the observations be consistent with model predictions, even though it could not be proved that the observations were due only to the prescribed CO<sub>2</sub> changes?

---

\* Corresponding author.

## 2. Introduction

We report on the results of a particular GCM study aimed at assessing the level of agreement between the observations and the CCM1 in making such predicted changes. To this end, a new simulation has been made with the assumed “pre-in-

dustrial” level of 265 ppm CO<sub>2</sub> suggested by Raynaud and Barnola (1985, which is lower than the more recently suggested value of 280 ppm); this can be compared with a previous simulation using a present-day level of 330 ppm (Oglesby and Saltzman, 1990,1992, hereafter O–S, 1990, 1992). Use is made of the O–S (1992) results pertaining to the

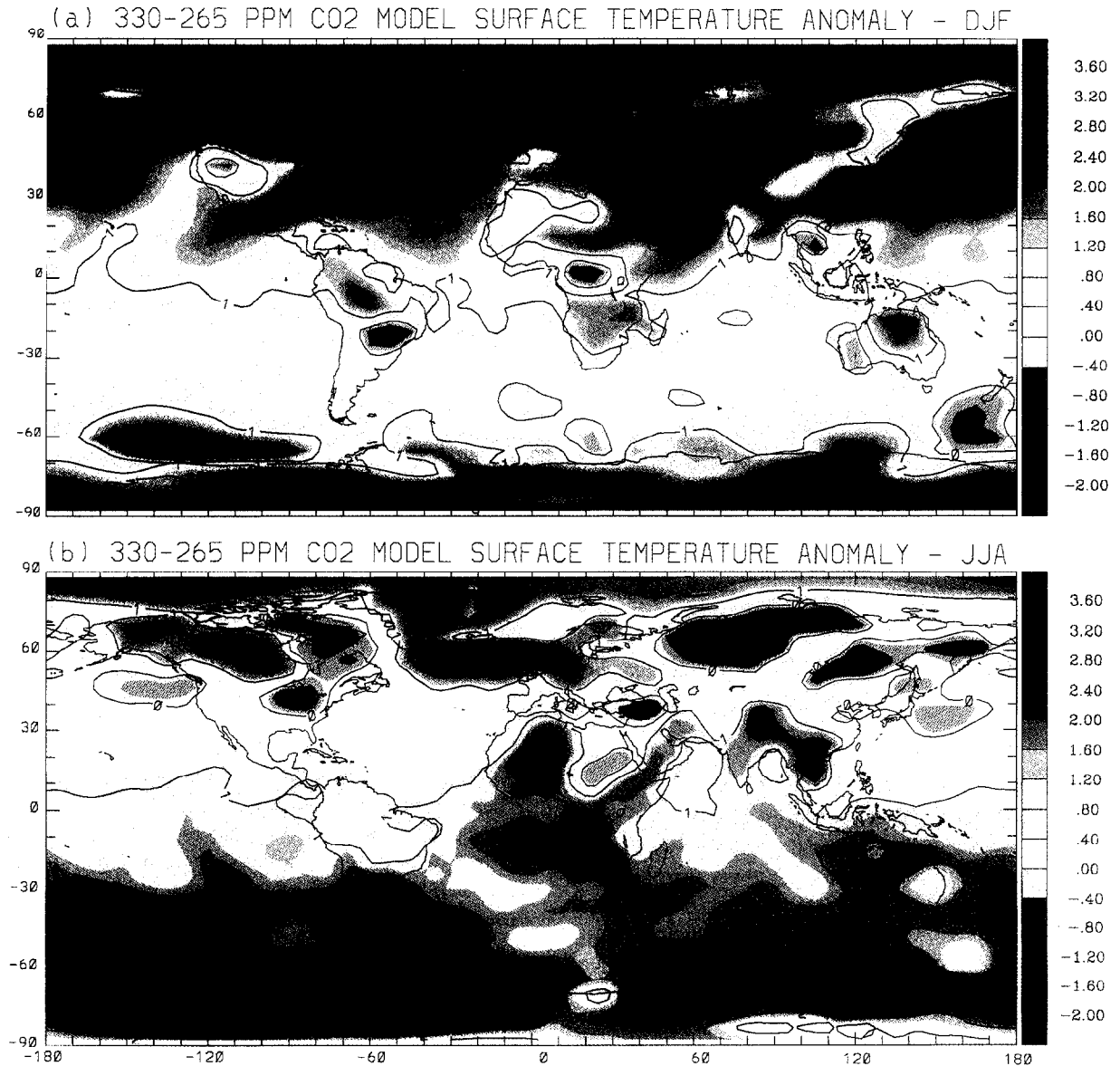


Fig. 1. Surface temperature differences (330 ppm minus 265 ppm CO<sub>2</sub>, colors as indicated in the key in °C) for (a) December, January and February (DJF) averages and (b) June, July and August (JJA) averages.

sensitivity of the GCM to a wide range of CO<sub>2</sub> changes (from 100 to 1000 ppm). O–S (1992) emphasized that their results were indicative of the climate sensitivity of “Planet CCM1” to changes in CO<sub>2</sub>. This new study, in essence, attempts to quantify the degree of similarity between Planet CCM1 and Planet Earth in this regard.

This GCM modeling combination included the National Center for Atmospheric Research (NCAR) Community Climate Model, version 1 (CCM1) coupled to a slab ocean/thermodynamic sea ice model based on Semtner (1976,1984). For more details on the models themselves see Williamson et al. (1987) and Covey and Thompson (1989); Williamson and Williamson (1987) and Randel and Williamson (1990) present the model statistics and discuss the strengths and weaknesses of the model. A thorough description of the CCM1 response to a wide range of CO<sub>2</sub> values and comparison to previous work is given in O–S (1992).

For the observations we use available surface temperature records (Jones and Briffa, 1992) to infer qualitative patterns and magnitude of changes that have occurred between 1890 and 1990. The sparseness of the observed dataset prohibits obtaining statistically reliable information prior to 1890 although one could resort to indirect measurements, principally from ice cores, to extend the observed record several centuries back in time. In addition, the need for a complete time record over the past century restricts our evaluation to 449 land and ocean points globally.

The radiation scheme for the present-day CCM1 control is initiated for the date 1975 AD, which corresponds to a concentration of 330 ppm, well below the current value (1990) of about 355 ppm. The differences in the model simulations (330 ppm minus 265 ppm) is actually less than our adopted current observed-minus-preindustrial difference of about 90 ppm (355–265 ppm). As noted above, the “pre-industrial” concentration of CO<sub>2</sub> may actually have been about 280 ppm (Siegenthaler and Oeschger, 1987; Neftel et al., 1982). However, it is advantageous to compare the 265 ppm case with the 330 ppm case since these values correspond well to the range of expected change in CO<sub>2</sub> concentration and are useful within the previous set of simulations (O–S, 1992; 265 ppm falls exactly halfway between

the previously made 200 ppm and 330 ppm simulations).

### 3. Results

#### 3.1. Comparison of the 265 ppm and 330 ppm simulations

We begin with a summary of the 330 ppm minus 265 ppm difference fields, for summer and winter, for each of the following basic variables: surface temperature, surface pressure, precipitation, storm tracks and sea ice coverage. These will be followed by a similar set of geographic maps of variables in the form of *t*-statistics.

#### Surface temperature

In Fig. 1(a,b) we show the 330 ppm minus 265 ppm difference in surface temperature for December, January, and February (DJF) and for June, July, and August (JJA). Considering first DJF, we find in the wintertime northern hemisphere a large warming exceeding 10° C over the North Atlantic and, to a lesser degree, over the North Pacific. In part, this is due to an overestimation of sea ice in the CCM1 control simulation and is discussed in a later section. Elsewhere, throughout most of the (wintertime) northern hemisphere midlatitudes the warming is between 2 and 5° C while in low latitudes and the summer southern hemisphere the warming, though generally uniform, is less than 2° C. A few gridpoints even show a slight cooling (< 1° C), although the area occupied by these is relatively small. The high latitude (wintertime) southern ocean experiences a strong warming, with elsewhere a more moderate warming of 2–4° C over Antarctica and the mid-latitude southern hemisphere. A general warming of about 2° C is found over the summer northern hemisphere, though fairly large regions (mostly over land) show instead a slight cooling. Based on these results, we can place the model response into two regimes: (1) A fairly high latitude, winter region with warming generally in excess of 5° C. (2) The summertime high latitudes and mid and low latitudes in both seasons, with warmings generally around 1–4° C.

### Surface pressure

O–S (1992) pointed out that, whereas surface temperature in CCM1 shows a fairly large response to CO<sub>2</sub> changes, the surface pressure anomaly of about 4–6 mb relative to the mean represents a

smaller percentage response to CO<sub>2</sub> changes. It is nonetheless of interest to compare the geographic distributions of surface pressures for the 265 ppm and 330 ppm simulations.

In Fig. 2(a,b) we show the 330 ppm minus 265

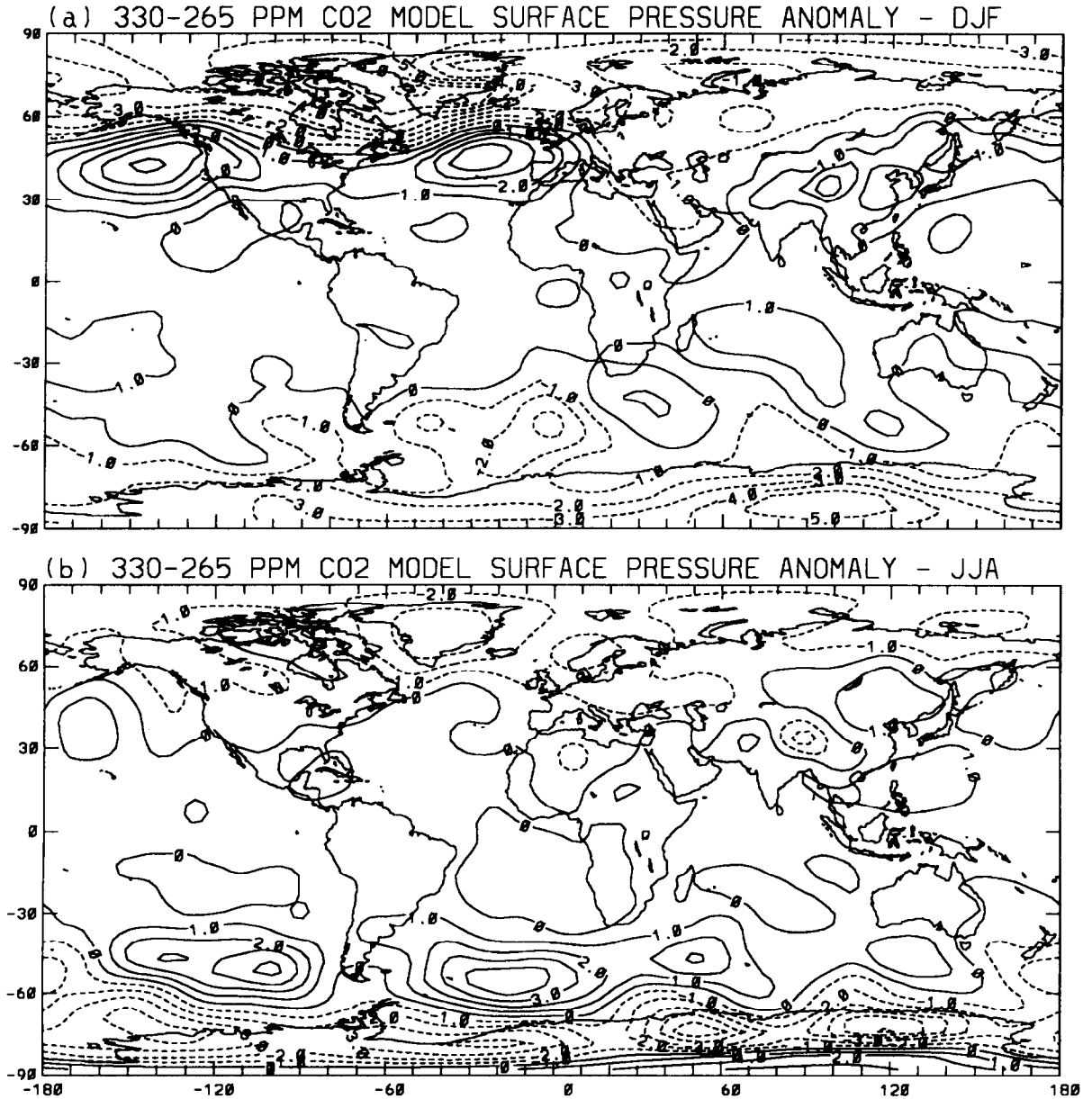


Fig. 2. Surface pressure differences (330 – 265 ppm CO<sub>2</sub> in mb) for (a) DJF and (b) JJA averages. Contours range from –10 to 5 with a contour interval of 1 mb.

ppm differences for DJF and JJA. The difference plots show the largest changes for both hemispheres in the wintertime mid and high latitudes, and much smaller changes in summer and low latitudes in both

seasons, broadly consistent with the results of O-S (1992). Generally, with the increase in CO<sub>2</sub> there is a decrease in the wintertime pressure gradient (i.e., the “highs” are lower and the “lows” are higher),

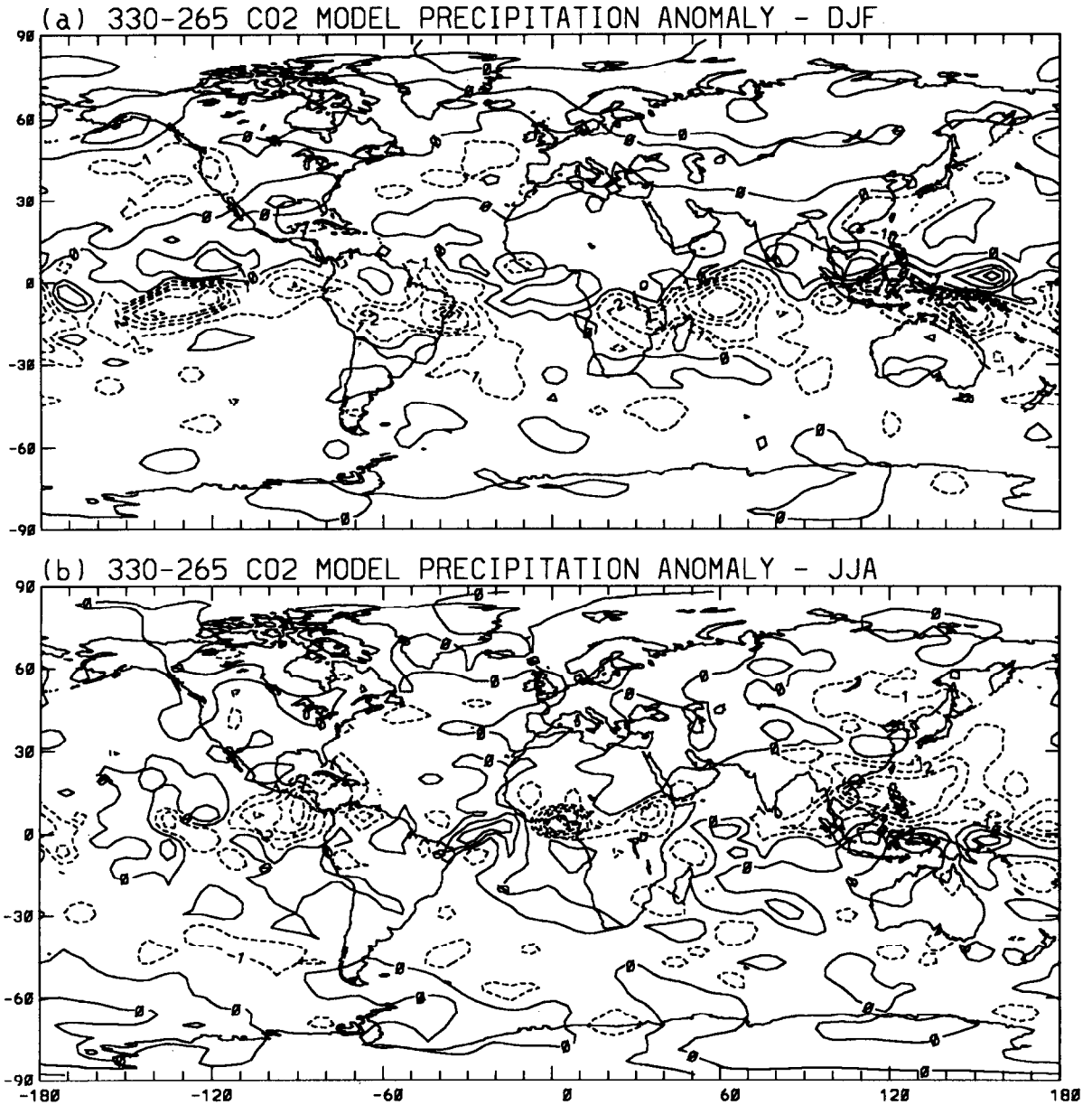


Fig. 3. Precipitation differences (330 – 265 ppm CO<sub>2</sub>, in mm d<sup>-1</sup>) for (a) DJF and (b) JJA averages. Contours range from -5 to 4 with a contour interval of 1 mm d<sup>-1</sup>.

possibly indicative of a decreased and poleward-shifted region of “storminess”, with relatively lower pressures at high latitudes (possibly decreasing the likelihood of cold air outbreaks). As described more

fully below, the largest pressure changes coincide for the most part with regions where sea ice also changes. Low-latitude and summertime surface pressures are generally higher over the oceans and lower over

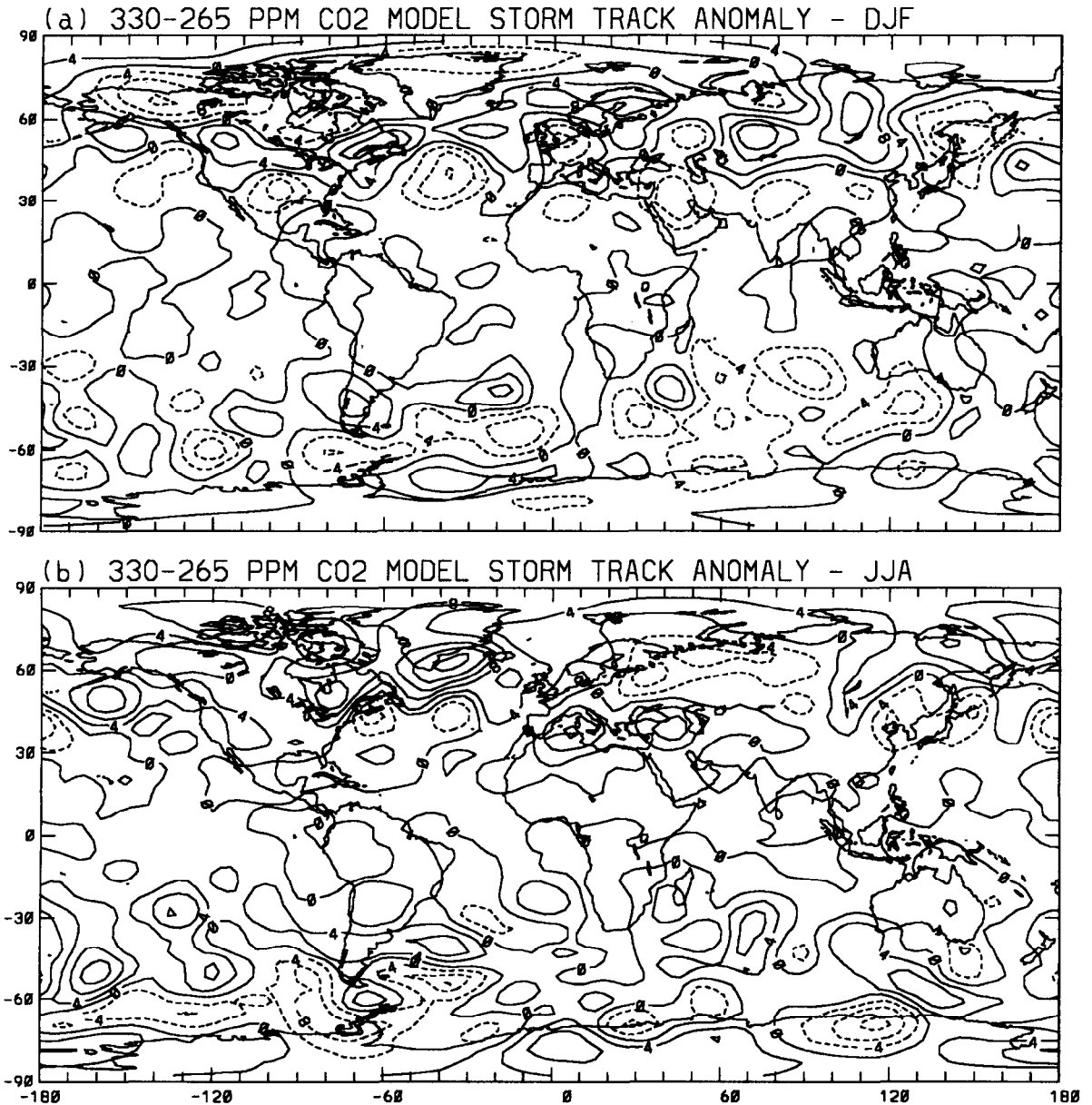


Fig. 4. Storm track indicator differences (330 – 265 ppm CO<sub>2</sub> in m) for (a) DJF and (b) JJA averages. Contours range from –20 to 20 with a contour interval of 4 m.

land, suggesting a slight increase in land–ocean pressure gradients and hence monsoonal flows, but the changes are not large or systematic.

### *Precipitation*

In Fig. 3(a,b) we show the 330 ppm minus 265 ppm difference in precipitation, again for DJF and JJA. Although precipitation is an inherently noisy field, some indication of patterns does emerge.

The tropical ITCZ appears to shift slightly northward in DJF, possibly reflecting more low-latitude surface heating at 330 ppm, although the simulation of this feature is crude in a low-resolution model such as the CCM (Randel and Williamson, 1990). In JJA, ITCZ precipitation appears to decrease over land regions and increase over the oceans. Elsewhere, the northern hemisphere land regions tend to show a slight increase in both seasons, except at higher latitudes and in southeast Asia. Precipitation over the adjacent oceans generally increases in winter (DJF) but decreases in summer (JJA). Though small, these changes are generally consistent with the trends noted by O–S (1992) for the much larger range of values from 100 ppm to 1000 ppm. The southern hemisphere poleward of about 15–20° S latitude shows no clear pattern of response in either season. We note that the slight increase in precipitation over northern hemisphere land areas with increasing CO<sub>2</sub> from 265 ppm to 330 ppm is similar to the conclusion of Groisman (1992) for observed precipitation trends over northern hemisphere land areas for the past 100 years. Both studies, however, note that these results may be at best marginally significant due to the high degree of variability in the patterns of precipitation.

### *Storm tracks*

The storm track index we use is the standard deviation of the band-pass filtered 500 mb geopotential height (Blackmon, 1986). The band-pass filter restricts the results to only those features on the synoptic scale of two to six days. Before we describe actual model results, we might first consider expectations based on the previous work of O–S (1992): (1) We might anticipate relatively small and statistically insignificant changes in storm tracks. (2) We might also expect that the major influences on such changes

would be due to changes in the distribution of sea ice.

In Fig. 4(a,b) we show the 330 ppm minus 265 ppm difference in the storm track index for both DJF and JJA. The most apparent feature is the validity of the first expectation, that is, the changes seem small overall and variable in nature, being of the order of at most a few meters. Nonetheless, several important features appear to be present. The North Atlantic storm track appears overall to be stronger at 330 ppm than at 265 ppm, despite the implications for greater baroclinicity at 265 ppm based on O–S (1992). Little difference between the two cases is seen in the North Pacific, although magnitudes there are slightly larger at 265 ppm. Given the fairly large year-to-year fluctuations in this quantity, however, not much significance can be attached to these results. An interesting feature of the difference plots is a northward shift in the storm track at 330 ppm in the North Atlantic and in the North Pacific in both the winter and summer seasons. This trend, though small and likely of marginal statistical significance, is consistent with the general southward shift of sea ice with decreasing CO<sub>2</sub>.

### *Sea ice*

A constantly recurring theme in the analysis of the results presented here as well as those of O–S (1992) is the importance of the areal extent of sea ice. The large response in surface temperatures over high latitude oceans noted in many CO<sub>2</sub> studies (including this one) is a result of the model sensitivity to the sea-ice albedo feedback. As noted by O–S (1992) the areas of largest sensitivity in surface temperature coincide with areas which change from ice-covered to ice-free. These areas correspond to the high latitude, winter regime (i) described in a previous section.

In Fig. 5 we show the range between winter and summer of sea ice area for (a) the northern hemisphere and (b) the southern hemisphere as simulated by O–S (1992) and this study. The figure also indicates, for reference, the climatological (observed) range in sea ice extent used by the standard CCM1 control (based on Levitus, 1982). A decrease in sea ice extent is seen in both hemispheres with an increase in CO<sub>2</sub> for both the minimum and maximum extents. Although the modeled scenario is for only a

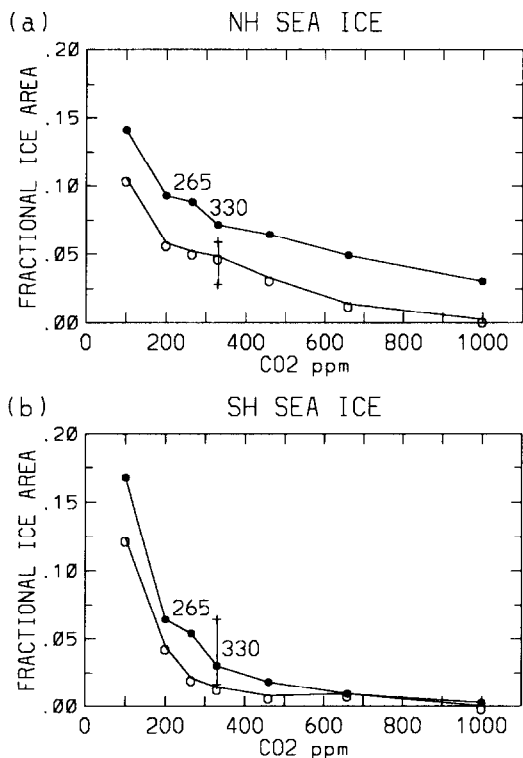


Fig. 5. Maximum (black circles) and minimum (open circles) seasonal sea ice extent for (a) the northern hemisphere and (b) the southern hemisphere for the combined results of this study and O-S (1992). The values are the fractional area of each hemisphere covered by sea ice. The 265 and 330 ppm values are labelled. The vertical solid lines denote the climatological range of seasonal sea ice extent from Levitus (1982).

small change in CO<sub>2</sub> (330 ppm minus 265 ppm), we still note a change in sea ice extent, particularly in winter. This is in contrast to the results of Chapman and Walsh (1993) who find a stronger decrease in the summertime rather than the wintertime Arctic sea ice extent for data spanning the past four decades. The O-S (1992) study indicated that changes in sea ice were larger with a decrease in CO<sub>2</sub> than were changes with a similar increase in CO<sub>2</sub> from present-day values. The results here also suggest that sea ice observations may be a key element in detecting short-term climatic changes, a point raised frequently before.

Several important caveats must be raised, however. First, our model simulations use a thermodynamic-only ocean and sea-ice component; in particular, no dynamical transports of heat by the ocean are

taken into account. One approximation frequently used with such models is to prescribe a horizontal heat flux "correction" that crudely accounts for such present-day heat transport. O-S (1992) made the choice not to use this for their simulations, arguing that since the heat-flux correction is determined for the present-day climate there was no way to determine how it would vary as CO<sub>2</sub> was changed. We continued this approach with the new 265 ppm simulation. This modeling approximation may enhance the sensitivity to sea ice (although it is not always clear what effect actual changes in heat transport might have), though as shown by O-S (1992, see Fig. 5) the seasonal cycle of sea ice in the northern hemisphere is reasonable in the 330 ppm control. It is also true that, for reduced CO<sub>2</sub> scenarios, use of present-day prescribed heat flux might artificially retard the growth of sea ice.

Second, although observations of present-day sea ice are improving with the use of satellites, studies such as Chapman and Walsh (1993) indicate that there is considerable year-to-year variability in sea ice extent. There is also disagreement in the analysis of observed changes in the Arctic. Chapman and Walsh (1993) find evidence of a decrease in sea ice extent corresponding to an increase in global temperatures, while Kahl et al. (1993) find no evidence of a significant trend in atmospheric temperatures in the Arctic. Although the modeled sea ice extent is larger than observed, the simulated change in sea ice extent is difficult to compare with observations due to the variability in the record. We chose not to emphasize the high latitude region in this study due to problems with both the modeled and observational record.

### 3.2. *T*-statistic for the 330 ppm minus 265 ppm results

To evaluate the significance of the 265 ppm minus 330 ppm changes, we rely primarily on a *t*-statistic, that is, the difference in the means normalized by the standard error of the model control as determined over a 15 year interval, and expressed in terms of confidence intervals. This test is only valid for climatic variables whose true distributions are generally Gaussian in nature. This is valid for many important variables such as surface temperature and pressure, but not for precipitation which is best

approximated by a chi-square distribution. We applied the  $t$ -statistic to the observational results as well, using the 1980s–1890s decadal differences divided by the standard error over the 100 year inter-

val. Comparison of the two  $t$ -statistics for the model and observed results may allow us to obtain a rough measure of the similarities and differences in areas of significant changes.

(a) 330–265 T-TEST STATISTIC SURFACE TEMPERATURE - DJF



(b) 330–265 T-TEST STATISTIC SURFACE TEMPERATURE - JJA



Fig. 6.  $T$ -test statistic for the 330 – 265 ppm  $\text{CO}_2$  surface temperature differences for (a) DJF and (b) JJA results. Color shadings indicate four regions with confidence levels: (i) 99% or greater (red), (ii) greater than 95% but less than 99% (yellow), (iii) greater than 90% but less than 95% (blue), and (iv) less than 95% (grey).

### Surface temperature

In Fig. 6(a,b) we show the 330 ppm minus 265 ppm differences presented as confidence levels determined by means of a simple student *t*-test. Shown are color shadings representing the 90%, 95%, and

99% confidence levels. Three features are of particular interest: (1) The wintertime mid and high latitudes in both hemispheres and the low latitude oceans in both seasons have changes that are significant almost everywhere to greater than 95%. (2) The

(a) 330-265 PPM T-TEST STATISTIC SURFACE PRESSURE - DJF



(b) 330-265 PPM T-TEST STATISTIC SURFACE PRESSURE - JJA



Fig. 7. *T*-test statistic for the 330 – 265 CO<sub>2</sub> surface pressure differences for (a) DJF and (b) JJA results. Contours are as in Fig. 6. Regions with confidence levels of 99% or greater are shaded.

summertime mid-latitude land regions and the North Pacific Ocean have changes that are not significant even at the 90% level. (3) A given region either demonstrates a change that is significant to better than 95% or that is not significant at all; there is little “grey area” where the statistical significance is not clear.

These tests, however, say nothing per se about the physical nature of the results. It is possible for isolated regions of one to several gridpoints to show a strong statistical significance without any particular physical meaning, while perhaps even more importantly, it is possible for large regions to show a systematic, physically plausible response that is at best marginally statistically significant due to large variability in these regions.

#### Surface pressure

In Fig. 7(a,b) we show the normalized differences as a *t*-test statistic at the 90%, 95%, and 99% confidence levels. The *t*-test results demonstrate a pattern that is considerably more complex than the pressure differences and the *t*-tests for surface temperature. While large regions show a response that is significant at up to 99% or greater, equally large regions do not show a significant response. Furthermore, unlike surface temperature, no clear pattern

emerges; the regions of systematic change noted in Fig. 2 do not show a coherent significance, with portions of each pressure change region being significant at 99% while other portions are not significant at all. We are left to conclude, as in O–S (1992), that the changes in Fig. 2 are likely to be physically meaningful, but small and difficult to distinguish from model variability. If we assume model variability is similar to observed variability (as we demonstrate in the next section is the case for surface temperature) then changes in surface pressure patterns that may actually have occurred during the recent past may be difficult to detect adequately even in a fairly long instrumental record.

#### 3.3. Comparison of 1980 minus 1890 observations

The most critical element in our analysis is the comparison of 330 and 265 ppm model results with observed climatic changes since the advent of the industrial age (circa 1800 AD). Unfortunately, we do not have reliable data as far back as 1800 AD; some gridded land and sea surface temperatures going back to about 1850 AD are available (see Farmer et al., 1989; Jones et al., 1991; Jones and Briffa, 1992; P. Jones, pers. comm., 1993). This dataset is a compilation of monthly mean surface air tempera-

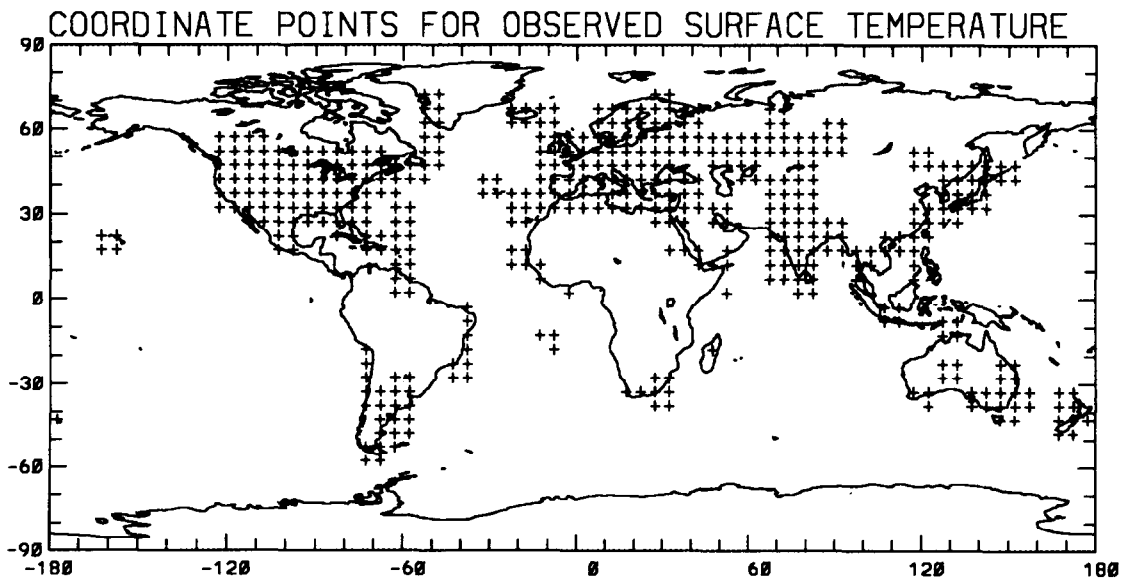


Fig. 8. Grid points of observed data.

tures based on meteorological station data and fixed-position weather ship data. These data, compiled by P. Jones, are available from the National Center for Atmospheric Research.

The requirement of quasi-continuous time series and reasonably widespread spatial coverage neces-

sary for a meaningful comparison of the observed and predicted temperature variations forces us to consider a more restricted data set of 449 land and ocean grid points (Fig. 8), located at  $5^\circ$  by  $5^\circ$  latitude–longitude intersections, representing the temperature anomalies going back only as far as

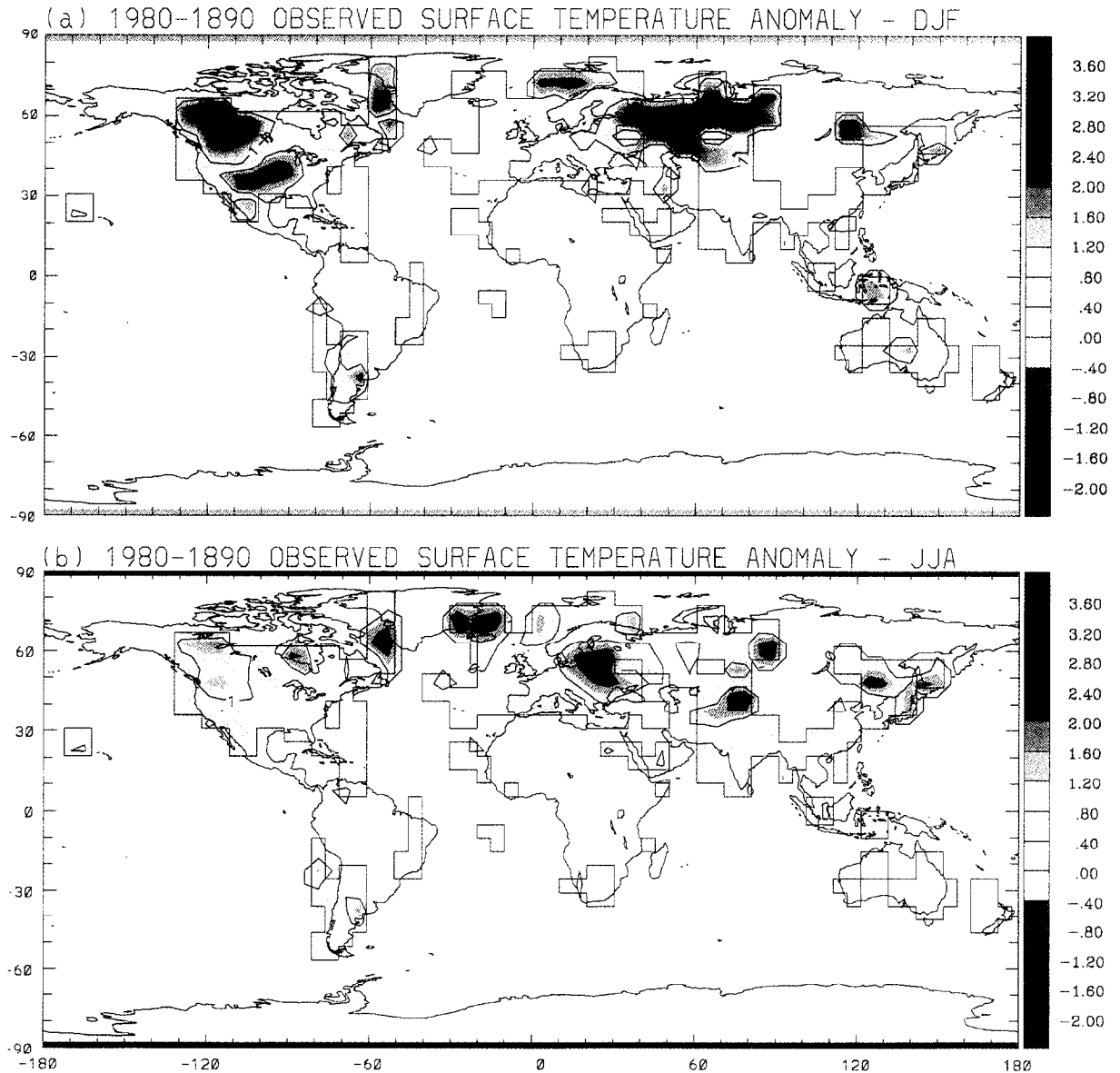


Fig. 9. Observed surface temperature anomaly (1980 – 1890, in  $^\circ\text{C}$ ) for (a) DJF and (b) JJA averages. Areas outside of grid boxes contain no data and are shown in white.

1890 AD. We crudely filter the data set by considering decadal means in order to mask the high frequency interannual and ENSO-type variability. The difference between the 1890s and 1980s decades is a rough measure of the temperature trend which can be compared to the CCM predictions.

#### Surface temperature

In Fig. 9(a,b) we show the 1980–1890 observed surface temperature anomaly for DJF and JJA. Even with the paucity of coverage these figures do show some broad similarities to the model results shown in Fig. 1. These observations show a warming in the wintertime northern hemisphere of 2–3°C, and a lesser warming in the summertime northern hemisphere of approximately 1°C over land areas with good coverage (i.e., North America and Europe). The warming indicated in the southern hemisphere land areas is about the same for the two seasons, approximately 1–2°C. The enhanced warming in the winter northern hemisphere, noted in the model results, is also evident in the observations. Although we do not see a similar warming in the winter southern hemisphere, we note that this is a region of sparse coverage and a smaller land area. We note also that the warming most evident in the observations occurs over areas of relatively good spatial and temporal coverage; North America and Europe.

Although there are some clear agreements on a more regional bases, we also note some disagreements; e.g., the observed winter cooling north of Scandinavia and to some extent in the central United States, as well as the summer cooling in the Denmark Strait and eastern European areas are not manifest in the model results. It may be of more significance, however, that the model has in fact predicted the existence of broad areas of cooling, in the face of a CO<sub>2</sub> increase, particularly in the northern hemisphere summer.

In Fig. 10 we show the globally-averaged trends in observed CO<sub>2</sub> and surface temperature and compare these to the model surface temperatures for the 265 and 330 ppm results. These plots indicate a clear association between the trends in CO<sub>2</sub> and the observed globally-averaged surface temperatures. The model results show a range of surface temperature similar to that seen in the observations for the period

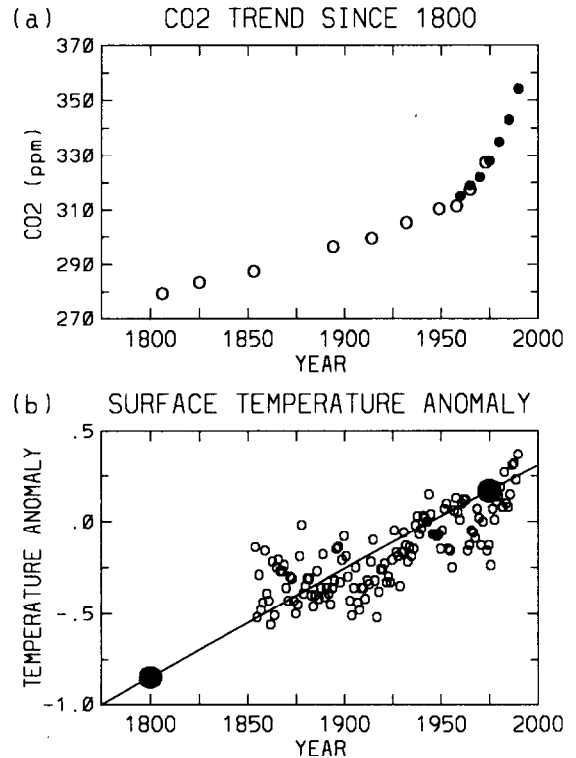


Fig. 10. Time series of (a) trend in atmospheric CO<sub>2</sub> (in ppm) over the last 200 years as reconstructed from ice cores (Jones et al., 1991), shown as open circles, and atmospheric CO<sub>2</sub> (in ppm) since 1960 as measured at Mauna Loa, Hawaii (Houghton et al., 1990), shown as black circles and (b) observed globally-averaged annual surface temperature anomaly (centered about the 1950–1970 temperature average, in °C, shown as open circles) and model globally-averaged annual surface temperature for the 265 ppm (assumed to correspond to approximately 1800) and 330 ppm (approximately 1975) CO<sub>2</sub> experiments (shown as the large black dots). The curve drawn in (b) indicates the functional relationship between surface temperature and CO<sub>2</sub> of O–S (1992).

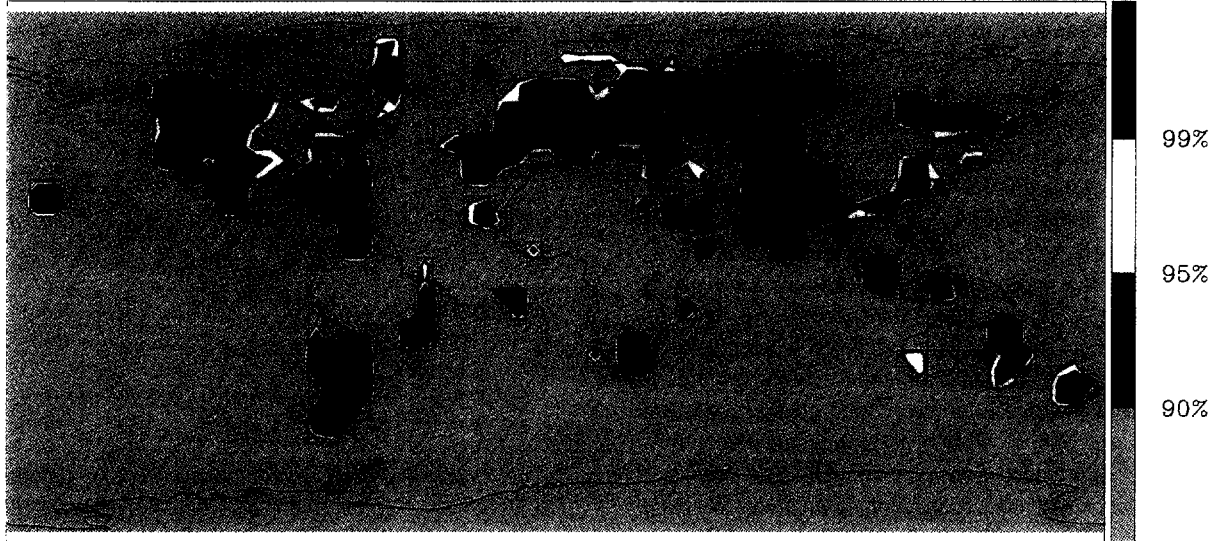
between 1850 and 1990 (corresponding to an approximate range in CO<sub>2</sub> from 287 to 340 ppm).

We note that in considering only CO<sub>2</sub> we are essentially ignoring the simultaneous increase in other greenhouse gases such as methane, nitrous oxide and CFCs. It follows, therefore, that our calculations of the effects of CO<sub>2</sub> alone must represent a lower bound to the full effects of the greenhouse gas increase. In this regard, a more appropriate quantity to consider would be the “equivalent CO<sub>2</sub>” (Houghton et al., 1990) for which we can expect a steeper

rise than shown for CO<sub>2</sub> alone in Fig. 10(a), and a somewhat more elevated position and greater slope of the line shown in Fig. 10(b). The need for these

corrections may be mitigated to some extent by the simultaneous increase in aerosols (see Erickson and Oglesby, 1992).

(a) 1980–1890 T-TEST STATISTIC SURFACE TEMPERATURE – DJF



(b) 1980–1890 T-TEST STATISTIC SURFACE TEMPERATURE – JJA



Fig. 11. *T*-test statistic for the 1980 – 1890 decadal temperature anomalies for (a) DJF and (b) JJA differences. Contours are as in Fig. 6 except that areas with no data are shown outside of grid boxes and are shaded grey.

### 3.4. *T-statistic for the 1980 (decadal) minus 1890 (decadal) observations*

#### *Surface temperature*

A *t*-statistic has been made of the decadal temperature anomalies for the period of 1890–1980. In Fig. 11(a,b) we show the *t*-test statistic, presented as confidence levels for the 1980 – 1890 observed surface temperature differences. The differences are shown to be significant almost everywhere there is data (North America and Europe) to greater than 99%. Over Europe, the summertime *t*-statistic map indicates some reduction in the areal coverage of the 99% confidence level, but this is not evident over North America. Indeed, for the observed dataset, the changes in surface temperature from the early industrial period to the present are highly significant for both seasons. These maps indicate the changes in observed surface temperature to be significant within this time period and outside of the realm of observed variability. The comparison of these maps to those of the *t*-statistic for the model results (Fig. 6) indicate some similarities in the areas of statistically-significant changes. This comparison suffers from the same problem as does the difference field comparison; the lack of complete coverage in the observations.

### 3.5. *Point-by-point correlation of modeled and observed surface temperature differences*

In order to make a quantitative statement about the similarity between the regional trends in the observational record and in the model we consider the linear correlation between the two sets of temperature difference maps shown in Figs. 1 and 9. We have interpolated the  $4.5^\circ \times 7.5^\circ$  CCM surface temperature grid onto a  $5^\circ \times 5^\circ$  map commensurate with the observational temperature anomaly grid. We then computed linear correlation coefficients for both the winter and summer difference maps using all 449 observational grid points with nearly continuous data. The confidence limits for the non-randomness of linear correlation coefficients *r*, under the assumption of non-autocorrelated data, are given by the probability distribution,

$$\Pr(r; \nu) = 1/\pi \{ \Gamma[(\eta + 1)/2] / \Gamma(\eta/2) \} \quad (1)$$

and are tabulated in many standard texts on statistics (e.g., Bevington, 1969).  $\Gamma$  is the gamma function and  $\eta$  represents the number of spatial degrees of freedom in the sample. For our case,  $\eta$  is quite a bit less than the nominal spatial sampling of 449 grid points used. A previous analysis (Mann and Park, 1993) estimating the length scale of short-range, frequency-independent correlations at roughly 1500 km predicts roughly 40 degrees of freedom present in our spatial sampling of the observational temperature anomaly field. We therefore use a value of  $\eta = 40$  for the effective number of degrees of freedom of the sample.

This point-by-point correlation allows us to compare the similarity between the relative regional trends in the model results and in the observations, yielding a correlation coefficient of 0.194 for the winter difference maps (explaining 4% of the variance) and a correlation of 0.129 for the summer difference maps (explaining 2% of the variance). While this explained variance is small, it should be noted that under the assumption of 40 degrees of freedom for the observed anomaly field (described above) this gives an 80% confidence limit for the non-randomness of the correlation between the wintertime maps, and roughly 55% confidence limit for the non-randomness of the correlation between the summertime maps. There appears to be a small, marginally significant correlation between the wintertime maps, and an even smaller, probably insignificant correlation between the summertime maps. These findings are consistent with the proposition that some of the variance in the observed regional trend of surface temperature anomalies might well be explained by the forcing and dynamics present in the model. The impact of the low resolution and subsequent distortion of topography in the CCM1, while difficult to quantify, also means that even in the most ideal case a correlation well less than 1.0 is the best that could be expected.

## 4. Summary and conclusions

We show the results of a modeling study which compares the results of a “present-day” climate of 330 ppm CO<sub>2</sub> to those of a “pre-industrial” climate simulation of 265 ppm CO<sub>2</sub>. The conclusions ob-

tained are similar to those of Oglesby and Saltzman (1992), who considered a much larger range of modeled CO<sub>2</sub> concentrations with the largest differences in surface temperature attributed to changes in snow and sea ice extent. The largest temperature changes, up to 10° C, are found in regions of the wintertime high latitude ocean. Regional changes in surface temperature between 2 and 5° C are noted in northern hemisphere winter mid-latitudes, with warmings of 1–2° C in summer northern hemisphere. *T*-test statistic results of the surface temperature difference fields indicate that large areas of the wintertime mid and high latitudes in both hemispheres show significant changes (greater than 99%).

In the O–S (1992) analysis the log sensitivity of the surface temperature and two formal measures of uncertainty were computed, the log misfit and the “jackknife” standard deviation, showing that regions of largest sensitivity also had the largest uncertainty. This is true for our results as well.

The model results show smaller changes in the precipitation and storm track indicator fields, as was suggested by the earlier study to a wider range of CO<sub>2</sub> concentrations (O–S, 1992). The present results indicate a slight northward shift in DJF of the tropical ITCZ and a JJA pattern of increasing precipitation over the oceanic portion of the ITCZ. Similarly, the storm track indicator shows only small changes in the 330–265 differences, although the North Atlantic storm track appears somewhat stronger in the 330 ppm simulation, contrary to the implications of the earlier study. In general, the storm track does seem to shift northward with increasing CO<sub>2</sub>, as would be indicated in the O–S results.

The changes described above occur within regions of much human activity and are significant within the realm of model sensitivity as indicated by the *t*-statistic. Subsequent comparison of observed surface temperature changes over the past century (of a similar time period as the prescribed CO<sub>2</sub> changes) show some similarities to the model results. The observations show a warming of approximately 2–3° C in the wintertime northern hemisphere, where data coverage is good. No similar warming is indicated in the winter southern hemisphere, where data coverage is especially sparse.

Analysis of the significance, using the *t*-statistic and a point-by-point correlation, suggest that the

observed 1980–1890 temperature differences are at least marginally significant in the wintertime northern hemisphere. Less significant are the summertime differences. The overall findings suggest that the model predictions are consistent with these observations and that some of the variance in the observed trend of surface temperature anomalies may be explained by the CO<sub>2</sub> forcing of the climate system, as represented by the CCM1. Both the model results and the observed regional patterns of change suggest that changes in surface temperature may be easier to detect over wintertime continents than summer. We cannot, however, rule out the possibility that a large part of the cause of the observed variability from 1800 (265 ppm) to 1975 (330 ppm) is due to low frequency internal variability. We are currently investigating this latter point by making and analyzing a series of very long (greater than 100 years) CCM1 simulations.

In these comparisons we consider only a single factor for explanation of the observed changes in surface temperature over the past 100 years, that of changing CO<sub>2</sub> concentration in the atmosphere. Conclusions of the statistical analyses indicate that this single factor (CO<sub>2</sub>) may account for some of the observed variance in the surface temperature, with statistical confidence of greater than 50% in both seasons. We note that in this study we compare the transient change in the observed climate to the equilibrium response of the modeled climate. It should be expected that the transient results will show climatic changes which are smaller in magnitude and highly variable compared to the equilibrium response. We see these expected results but also note these changes are significant within the realm of the natural variability.

Our analysis concentrates on the mid-latitudes where both observed coverage and model reliability are good. High latitude regions which generally show a large response to modeled CO<sub>2</sub> changes are not central to our analysis because these regions show a high degree of variability in year-to-year observations and a high model uncertainty (Chapman and Walsh, 1993; Oglesby et al., 1994). Oglesby et al. (1994) suggest that low latitude regions may show small, but statistically significant, changes in climate. However, these regions lack sufficient temporal and spatial coverage for this analysis.

## 5. Epilogue

Imagine now that it is the year 1990, in which CO<sub>2</sub> levels are known to have risen well above even 330 ppm (~360 ppm). You find a trunk in your attic, inside of which you find a precious paper from 1800 AD reporting on the results of these 265 ppm and 330 ppm simulations with CCM1. You then compare these results with the just published Jones et al. (1991) dataset. What would you conclude, and what would you think of the veracity of the “prediction” made 190 years earlier? We suspect that you would believe the predictions made were not without at least some merit.

## Acknowledgements

This research has been supported by the Electric Power Research Institute (EPRI), Contract No. 2333-11 at Yale University as part of the Model Evaluation Consortium for Climatic Assessment (MECCA), and by the Department of Energy grant DE-FG02-85ER14144 to W. Prell, J. Kutzbach, R.J. Oglesby and T. Webb. Partial support was also provided by the Climate Dynamics Program of the National Science Foundation under grant ATM-9222591 to Yale University and by the Climate and Global Change Program of the National Oceanic and Atmospheric Administration under grant NA36GP0396 to the University of North Carolina at Charlotte and Scripps Institution of Oceanography. The computations were made at the National Center for Atmospheric Research (NCAR), which is sponsored by the National Science Foundation, with computing grant 36211011 from the NCAR Scientific Computing Division. Additional computational support was provided under the MECCA program. The suggestions of two anonymous reviewers were appreciated.

## References

- Bevington, P.R., 1969. *Data Reduction and Error Analysis for the Physical Sciences*. McGraw-Hill, New York, 336 pp.
- Blackmon, M.L., 1986. Building, testing and using a general circulation model. In: J. Willebrand and D.L.T. Anderson (Editors), *Large-Scale Transport Processes in Oceans and Atmospheres*. Reidel, Dordrecht, pp. 1–70.
- Chapman, W.L. and Walsh, J.E., 1993. Recent variations of sea ice and air temperature in high latitudes. *Bull. Am. Meteorol. Soc.*, 74: 33–47.
- Covey, C. and Thompson, S.L., 1989. Testing the effects of ocean heat transport on climate. *Global Planet. Change*, 75: 331–341.
- Erickson III, D.J. and Oglesby, R.J., 1992. Sensitivity tests of climate models to perturbations in cloud albedo from anthropogenic sulfur. *EOS*, 73: 71.
- Farmer, G., Wigley, T.M.L., Jones, P.D. and Salmon, M., 1989. Documenting and explaining recent global-mean temperature changes. In: *Final Rep. Nat. Environ. Res. Council. Contract no. GR3/6565*, 141 pp.
- Groisman, P.Y., 1992. Studying the North American precipitation changes during the last 100 years. In: *9th Int. Meet. Statist. Climatol.*, Toronto, June 21–26, 1992.
- Houghton, J.L., Jenkins, G.J. and Ephraums, J.J. (Editors), 1990. *Climate Change. The IPCC Scientific Assessment*. Cambridge Univ. Press.
- Jones, P.D. and Briffa, K.R., 1992. Global surface air temperature variations during the 20th century: Part I—Spatial, temporal and seasonal details. *Holocene*, 1: 165–179.
- Jones, P.D., Raper, S.C.B., Cherry, B.S.G., Goodess, C.M., Wigley, T.M.L., Santer, B., Kelley, P.M., Bradley, R.S. and Diaz, H.F., 1991. An updated global grid point surface air temperature anomaly data set: 1851–1990. *NDP-020/R1. Carbon Dioxide Inf. Anal. Center, Oak Ridge Natl. Lab., Oak Ridge, TN*, 346 pp.
- Kahl, J.D., Charlevoix, D.J., Zaitser, N.A., Schnell, R.C. and Serreze, M.C., 1993. Absence of evidence for greenhouse warming over the Arctic Ocean in the past 40 years. *Nature*, 361: 335–336.
- Levitus, S., 1982. *Climatological Atlas of the World Ocean*. NOAA Prof. Pap., 13, 173 pp.
- Mann, M.E. and Park, J., 1993. Spatial correlation of interdecadal variation in global surface temperatures. *Geophys. Res. Lett.*, 20: 1055–1058.
- Neftel, A., Oeschger, H., Schwander, J., Stauffer, B. and Zumbunn, R., 1982. Ice core sample measurements give atmospheric carbon dioxide content during the past 40,000 years. *Nature*, 295: 220–223.
- Oglesby, R.J. and Saltzman, B., 1990. The sensitivity of equilibrium surface temperature in a GCM to systematic changes in atmospheric carbon dioxide. *Geophys. Res. Lett.*, 17: 1089–1092.
- Oglesby, R.J. and Saltzman, B., 1992. Equilibrium climate statistics of a GCM as a function of atmospheric CO<sub>2</sub>: I. Geographic distributions of primary variables. *J. Climate*, 5: 66–92.
- Oglesby, R.J., Marshall, S., Larson, J. and Saltzman, B., 1994. A comparison of GCM Sensitivity to CO<sub>2</sub> and solar constant changes. In: *Proc. 6th Conf. Climate Variations, AMS, January 23–28, 1994, Nashville, TN*, pp. 91–95.
- Randel, W.J. and Williamson, D.L., 1990. A comparison of the climate simulated by the NCAR Community Climate Model (CCM1:R15) with ECMWF analyses. *J. Climate*, 3: 608–633.
- Raynaud, D. and Barnola, J.M., 1985. An Antarctic ice core reveals atmospheric CO<sub>2</sub> variations over the past few centuries. *Nature*, 315: 309–311.

- Semtner, A., 1976. A model for the thermodynamic growth of sea ice in numerical simulations of climate. *J. Phys. Oceanogr.*, 6: 379–389.
- Semtner, A., 1984. On modelling the seasonal thermodynamic cycle of sea ice in studies of climatic change. *Clim. Change*, 6: 27–37.
- Siegenthaler, U. and Oeschger, H., 1987. Biospheric CO<sub>2</sub> emissions during the past 200 years reconstructed by deconvolution of ice core data. *Tellus*, 39B: 140–154.
- Williamson, D.L., Kiehl, J.T., Ramanathan, V., Dickinson, R.E. and Hack, J.J., 1987. Description of NCAR Community Climate Model (CCM1). NCAR Tech. Note NCAR/TN-285 + STR, 112 pp.
- Williamson, G.S. and Williamson, D.L., 1987. Circulation statistics from seasonal and perpetual January and July simulations with NCAR Community Climate Model (CCM1): R15. NCAR Tech. Note NCAR/TN-302 + STR, 199 pp.